POLITECNICO DI TORINO
Repository ISTITUZIONALE

Temperature Distribution Mapping Using an FBG-Equipped Probe for Solid Tumor Laser Ablation

Original
Temperature Distribution Mapping Using an FBG-Equipped Probe for Solid Tumor Laser Ablation / Gassino, Riccardo; Pogliano, Jennifer; Perrone, Guido; Vallan, Alberto. - STAMPA. - (2018), pp. 73-78. (Intervento presentato al convegno 13th IEEE International Symposium on Medical Measurements and Applications, MeMeA 2018 tenutosi a Roma nel 11-13 giugno 2018).

Availability:
This version is available at: 11583/2710327 since: 2018-06-29T10:01:36Z

Publisher:
IEEE Institute of Electrical and Electronics Engineers Inc.

Published
DOI:

Terms of use:

This article is made available under terms and conditions as specified in the corresponding bibliographic description in the repository

Publisher copyright

(Article begins on next page)

12 October 2024

Temperature Distribution Mapping Using an FBG-Equipped Probe for Solid Tumor Laser Ablation

Riccardo Gassino, Jennifer Pogliano, Guido Perrone and Alberto Vallan
Politecnico di Torino
Torino, Italy
Email: alberto.vallan@polito.it

***Abstract*—In recent years, laser ablation treatments have become promising therapies for early-stage solid tumors, although the anatomical variability within the irradiated organs (i.e., presence of blood vessels and other inhomogeneities) greatly challenges the control of the tissue temperature throughout the medical procedure and thus the optical therapeutic outcome. To help getting around these limitations, a new fiber optic probe able to both deliver the laser light with optimal irradiation pattern and measure the temperature in the tumor region had been previously developed. This paper, using simulations validated with experimental data, aims at demonstrating how this probe, combined with suitable hyperthermal treatment planning, can be used to overcome the discrepancies between ex-vivo and in-vivo laser ablation procedures.**

I. Introduction

The increasing demand for minimally invasive cancer treatment procedures, along with the continuous technological progress in applied electromagnetics, have made solid tumor thermal ablation a viable alternative to surgical resection, especially in the treatment of malignancies in the liver, pancreas [1], kidney [2], bone [3], and lung. The effectiveness of such procedures relies on the ability of high temperatures to irreversibly damage biological cells. Depending on the particular thermal ablation procedure, the absorption of certain electromagnetic waves (radio frequency waves, leading to Radio-Frequency Ablation, RFA, microwaves leading to MicroWave Ablation, MWA, or laser light, leading to Laser Ablation, LA) results in a heat generation within the tissue, with a consequent increase in the temperature [4], [5]. The treatment is successful (i.e., the cancer cells are destroyed) if the tissue temperature locally increases above a certain cytotoxic level – about $55\,^{\circ}\mathrm{C}$ – that ensures the onset of cellular coagulative necrosis in few minutes.

Considering deep-laying organs, such as liver or pancreas, the electromagnetic energy has to be percutaneously delivered through a suitable applicator. The combination of laser light and optical fiber delivery probes is particularly interesting because of the advantages of LA [6], [7] and of the all-dielectric nature and small size of the resulting applicator [8]. For the treatment to be effective and safe, the tissue temperature during the entire procedure should stay in the $60\,^{\circ}\mathrm{C}$ to $85\,^{\circ}\mathrm{C}$ range in the entire tumor mass region. As a general rule, the higher the temperatures, the shorter the treatment time; however, temperature values significantly higher than $100\,^{\circ}\mathrm{C}$ should be avoided, as they may cause tissue carbonization. Indeed, besides for releasing possible toxic residues, charred regions have higher absorption than that of the surrounding tissue, leading to strong temperature distribution distortions.

To optimize the treatment with respect to the tumor shape, different Hyperthermal Treatment Planning (HTP) tools have been developed in the past in order to estimate, a priori, the process parameters required to produce the required cytotoxic temperature distribution. Most of the HTPs are for RFA and MWA [9], the two first and therefore most common ablation modalities, although some specific for LA are starting to appear [10].

HTPs are valuable tools, although different sources of uncertainty degrade their reliability, the most relevant being the great variability in the anatomy of the organ receiving the therapy, which can significantly affect the temperature distribution. For example, changes in the tissue composition may produce localized absorptions (heat sources), while large blood vessels may locally reduce the temperature (heat sinks) [11]. Therefore, to ensure optimal outcomes, the HTP should be updated in real-time following the continuous temperature mapping during the heating process. In general, these temperature distribution measurements can either be achieved through imaging techniques (e.g., Magnetic Resonance Imaging, MRI, Computerized Tomography, CT, or Ultra-Sounds, US) or by using multiple sensors (only fiber sensors because the presence of laser irradiation prevents the use of metallic temperature sensors, such as thermocouples) at different locations. Unfortunately, none of these solutions is fully adequate: imaging monitoring is expensive, may lead to artifacts and is not always available, whereas the use of temperature sensors requires performing further percutaneous insertions, therefore increasing the invasive impact. Moreover, when dealing with multiple percutaneous insertions, it is very difficult to precisely maintain the relative positions between the sensors as defined during the treatment planning phase; and this may lead to non negligible errors due to the large gradients typically present during LA procedures. Therefore, the ideal solution would be to have the possibility to update the HTP using temperature readings at the applicator position only; this can be done using a probe structure that embeds standard Fiber Bragg

Gratings (FBGs) as all-dielectric temperature sensors since they are among the most reliable solutions in biomedical applications [12], [13]. A more recent alternative currently being explored in the literature is to use chirped FBGs for temperature distribution monitoring [14]–[16].

In previous papers we have already proposed a fiber optic applicator with both laser delivery and temperature sensing capabilities [8], [17], [18]. The sensing is entrusted to one or more FBGs, which are directly inscribed in the delivery fiber core or bundled together with the delivery fiber, thereby in both cases preventing the need to perform further penetrations. Moreover, the developed probe has a customized irradiation pattern that can be adapted to match the tumor shape.

A first step towards the development of a HTP integrated with temperature measurements taken along the probe position is the development of a suitable model to analyze the impact of tissue inhomogeneities on the readings of remotely located sensors. With this objective, the paper firstly reports on the validation of the probe irradiation model by comparing simulations carried out with a Finite Element Method (FEM) software tool with experiment on an ex-vivo animal liver; then, analyzes the effects of blood perfusion during in-vivo laser ablation procedures using the validated model. Finally, it demonstrates that it is possible to relate the temperature distribution throughout the targeted region with the temperature values read by the FBG sensors positioned along the irradiating delivery fiber.

II. Fiber optic tool

Currently, laser ablation is mainly performed using a flat tip fiber from which the light exits forming a cone, having vertex angle set by the fiber numerical aperture. This results in a high energy absorption occurring in the very first portion of the tissue and a consequent hot-spot formation. This effect may be limited by adopting a different optical fiber configuration, capable of a broader and more uniform temperature distribution [17]. Such a probe is based on a double-cladding fiber that, in addition to the previously mentioned built-in sensing capability, displays, in the last few millimeters of its length, a set of grooves achieved with a surface micro-patterning process. These grooves are induced on the fiber surface, stripped of its outer polymeric cladding, via a CO_2 laser irradiation. The intent of this procedure is to obtain a diffused irradiation pattern that surrounds the entire fiber end portion. Furthermore, as the surface micro-patterning may be customized, it is possible to match the specific needs of the ablation procedure. In the particular case considered in this paper, the grooves have depth and position chosen to produce a uniform irradiation pattern and thus a uniform thermal distribution along the fiber axis for a length of approximately $1.5\,\mathrm{cm}$. This required non uniformly distributing a set of grooves over a $1\,\mathrm{cm}$ length, at three different angular locations ($0°$, $120°$ and $240°$). In order to analyze different FBG sensors positions with respect to the irradiation pattern, for the experimental part, the sensors ($3\,\mathrm{mm}$ long and $5\,\mathrm{mm}$ spaced FBGs) were inscribed in a separate fiber located in close proximity of one side of the modified region of the irradiating fiber.

III. Validation of the laser ablation model

A. The model

As a preliminary study, ex-vivo experiments may provide useful information regarding the effects of the ablation procedure. Nevertheless, a careful treatment planning must also consider the differences between ex-vivo and in-vivo organs, which greatly influence the outcome of the treatment. Indeed, the two situations largely differ: an ex-vivo liver, for instance, cannot account for the effect of blood perfusion, which actually constitutes a heat sink phenomenon during the thermal ablation procedure in in-vivo organs; likewise, metabolic heat rates are also absent in an ex-vivo experiment. The chosen roadmap started from developing a model that takes into account the complexity of an in-vivo liver, validated in a preliminary step by ex-vivo experiments. The simulations are carried out using a FEM tool, which couples a ray tracing study (optical problem) to a heat conduction analysis (thermal problem) for ex-vivo cases and to the bio-heat equation (thermal problem with perfusion and metabolic heat rate) for in-vivo cases [19]. The ray tracing algorithm describes the propagation of light in terms of rays traveling in straight lines in homogenous media and having paths governed by the laws of reflection and refraction at interfaces between different media. Light experiences negligible losses as it is guided along the fiber and is instead readily absorbed once it encounters a lossy medium, such as the biological tissue. Light absorption – taken into account through the imaginary part of the refractive index – results into a heat generation within the tissue and a consequent temperature rise in the surroundings. Heat conduction is governed by the following equation:

$$\rho c_{\mathrm{p}} \frac{\partial T}{\partial t} = \nabla \cdot (k \nabla T) + Q_{\mathrm{laser}} \tag{1}$$

where ρ, c_{p} and k are, respectively, the medium density, specific heat and conductivity, and Q_{laser} is the power source term that takes into account the laser light absorption in the medium. The bio-heat equation has much in common with the previously discussed equation but, in addition, accounts for the perfusion action of veins and arteries within the targeted domain, as well as for the metabolic heat rate:

$$\rho c_{\mathrm{p}} \frac{\partial T}{\partial t} = \nabla \cdot (k \nabla T) + Q_{\mathrm{laser}} + \omega_{\mathrm{b}} c_{\mathrm{b}} \rho_{\mathrm{b}} (T - T_{\mathrm{b}}) + Q_{\mathrm{m}} \tag{2}$$

where ρ_{b}, c_{b}, ω_{b} and T_{b} are, respectively, the blood density, specific heat, perfusion rate and average temperature: these are the quantities needed to evaluate the blood perfusion effect. Q_{m} models the heat source due to metabolic processes.

The metabolic heat rate is usually considered to be negligible, whereas the blood perfusion deeply affects the treatment. Specifically, blood perfusion has the effect of producing a general cooling of the treatment environment and leads to distortions in the otherwise uniform thermal distributions

obtained in laser ablation. As these non-uniformities are not easily predictable, it is useful to rely on computational tools in order to simulate the effect of such distortions on the heating process.

B. Ex-vivo experiment

The model introduced above was preliminary validated in an ex-vivo case to assess its capability to correctly predict the affected tissue area and the maximum achieved temperatures. To provide a reference case the developed fiber optic applicator was used to irradiate a portion of swine liver with $4\,\mathrm{W}$ of laser light at $915\,\mathrm{nm}$ for ten minutes. Fig. 1 shows the resulting ablation injury, recognizable as a pale pink elliptical mark in the tissue.

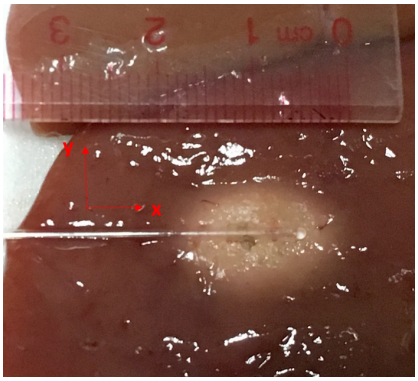

Fig. 1. Ablation injury after ten minutes irradiation with $4\,\mathrm{W}$ laser power.

The ablation mark interests approximately $1.5\,\mathrm{cm}$ in the horizontal direction. Temperatures were monitored in real time throughout the experiment via a thermal camera to have a map of the entire distribution. In order to have a better grasp of the actual temperatures in the immediate vicinity of the applicator, the experiment was carried out by sandwiching the fiber between two slices of liver; then, the upper slice was removed immediately before recording the thermal camera results, so that the retrieved information could be as little affected by air convection phenomena as possible. Fig. 2 and Fig. 3 show the thermal camera measurements after $10\,\mathrm{min}$ of laser irradiation. In order to match the temperatures used in actual thermal ablation procedures, the liver was conveniently placed over a hot plate, which ensured an initial temperature of about $37\,^{\circ}\mathrm{C}$.

C. Model validation

Once the experimental data had been obtained, a FEM-based software was used to simulate the above experiment in order to validate the simulation approach and tune the liver absorption parameter with respect to the nominal data found in the literature. As previously mentioned, a ray tracing algorithm was applied to study the behavior of the laser light from its generation to its absorption in the organ. Light attenuation within the tissue results in a generation of heat, which then diffuses to the surroundings mainly through conduction phenomena. The heat conduction equation was thus applied to our

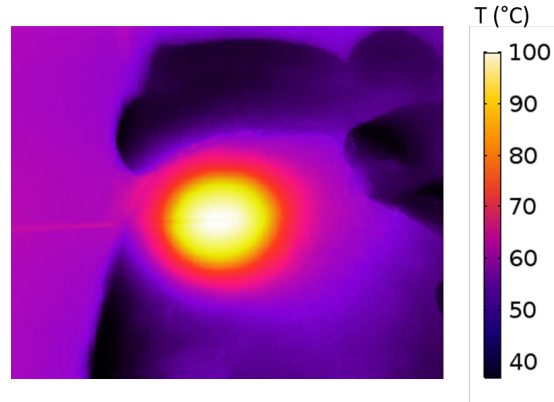

Fig. 2. Thermal camera image of the experiment in Fig. 1. The fiber probe is visible in the left-hand side of the picture.

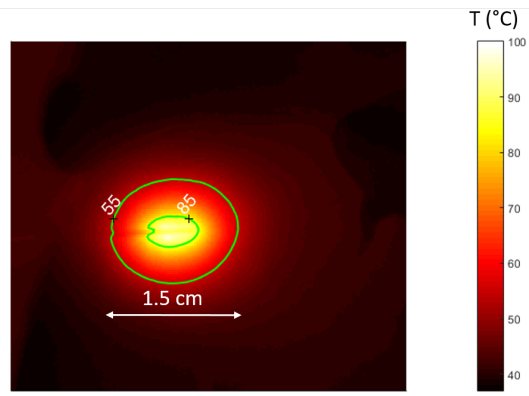

Fig. 3. Thermal camera image of the experiment in Fig. 1 with evidenced the $55\,^{\circ}\mathrm{C}$ and $85\,^{\circ}\mathrm{C}$ isothermal curves.

model. The parameters (in terms of fiber irradiation pattern, laser power and treatment time) used for the experiment were maintained in the simulation. The simulated temperature map is reported in Fig. 4.

The effect of the irradiation is to create a high temperature zone of more or less $1.5\,\mathrm{cm}$ in the horizontal direction, which is centered in the mid-point of the fiber active length. In this region, temperatures higher than $55\,^{\circ}\mathrm{C}$ are reached and this is in good agreement with the measurement results obtained with the thermal camera. Fig. 4 shows that, in the absence of blood perfusion, the temperature distribution obtained with laser irradiation is symmetrical, as expected from experiments. Also, the temperature read by the grating sensors during the experiment was in very good agreement with that predicted by the simulations for the same locations.

IV. Analysis of in-vivo simulated ablation

Given the excellent results obtained with the model for the ex-vivo case, the next step was then to simulate an in-vivo laser ablation procedure by applying the bio-heat equation to the domain, instead of the heat transfer in solids. Tab. I provides a

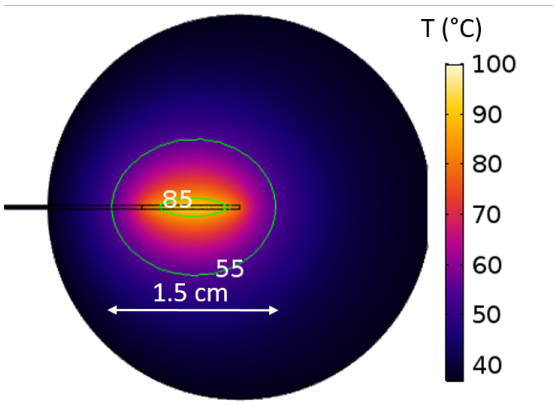

Fig. 4. Surface temperature in simulated ex-vivo liver with evidenced the 55 °C and 85 °C isothermal curves.

TABLE I
SUMMARY OF THE PARAMETERS USED TO MODEL THE BLOOD PERFUSION.

w_b	$0.064\,1/\mathrm{s}$
C_b	$4180\,\mathrm{J/kgK}$
ρ_b	$1000\,\mathrm{kg/m^3}$
T_b	$37\,°\mathrm{C}$
Q_met	$0\,\mathrm{W/m^3}$

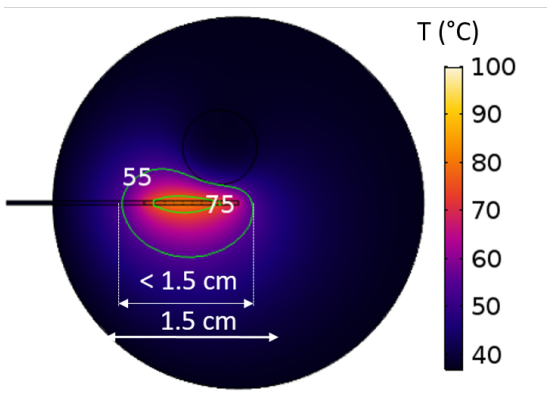

Fig. 5. Surface temperature in simulated in-vivo liver with evidenced the 55 °C and 75 °C isothermal curves.

summary of the values used to model the blood perfusion [20]. The metabolic heat rate was assumed to be negligible [21].

In order to demonstrate the effect of blood vessels and the impact of perfusion, in the example here reported, a case of tumor ablation near a $8\,\mathrm{mm}$ (diameter) vessel - similar to the hepatic artery - was simulated. The resulting temperature map obtained after $10\,\mathrm{min}$ irradiation is reported in Fig. 5.

The temperature distribution clearly shows a distortion caused by the presence of a large blood vessel in the proximity of the fiber tip, which acts as a heat-sink. Moreover, as Fig. 5 shows, accounting for blood perfusion leads to a general temperature decrease with respect to the ex-vivo simulation and this reduces the area with temperature higher than $55\,°\mathrm{C}$, the value assumed to be the limit for a safe ablation within the considered time frame.

A. Discussion

It is possible to compare the ex-vivo and in-vivo simulations by considering the temperature evolution in the two situations in a fixed point in between the applicator and the blood vessel, such as the one plotted in Fig. 6. Fig. 7 shows the temperature evolutions in ex-vivo (no perfusion) and in-vivo (perfusion) cases: it can be seen that the presence of the blood vessel in the in-vivo simulation results in a temperature decrease of about $20\,°\mathrm{C}$. The value at this point is still higher than the cytotoxic value, so tumor cells at that location would ideally be killed; however, clearly, a reduction of the overall temperature implies a reduction of extension of the area in which the tumor cells are destroyed.

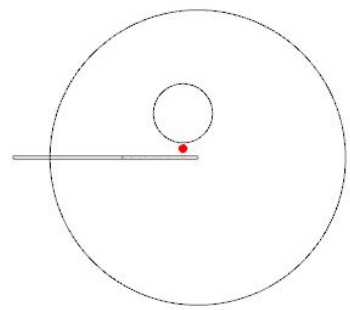

Fig. 6. Considered simulation geometry: the red dot marks the location where the temperature evolutions in ex-vivo and in-vivo simulations were compared.

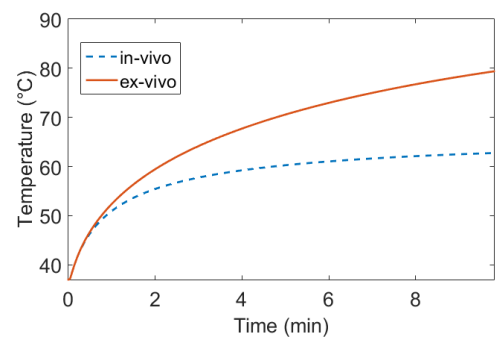

Fig. 7. Temperature evolution in ex-vivo and in-vivo simulations. The presence of the blood vessel in the in-vivo simulation results in a temperature decrease of about $20\,°\mathrm{C}$.

The temperature decrease can be counteracted by increasing the power until cytotoxicity is reached everywhere within the target, while avoiding to largely exceed $100\,°\mathrm{C}$ for the maximum temperature. Running several simulations, it turned out that in the considered example with $5.5\,\mathrm{W}$ it is possible to obtain a temperature distribution that closely matches that of the ex-vivo case; the resulting temperature distribution is shown in Fig. 8.

A better evaluation of the previous results may be obtained by analyzing the temperature in the reference point in Fig. 6

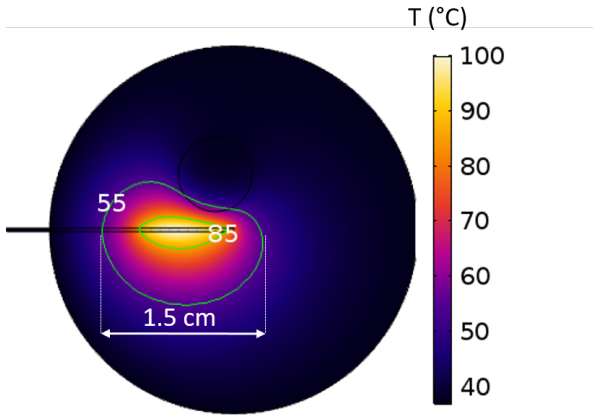

Fig. 8. Surface temperature in simulated in-vivo liver with higher laser power to counteract the effect of the blood vessel.

for the three possible cases: no perfusion, perfusion at 4 W and perfusion at 5.5 W (Fig. 9).

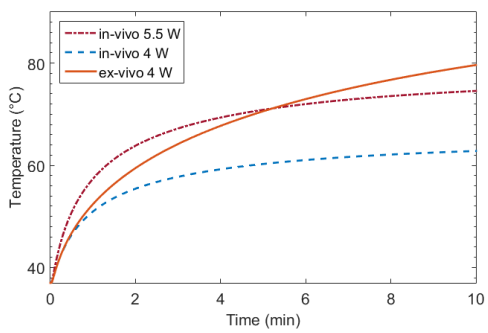

Fig. 9. Temperature evolution at the reference point (red dot in Fig. 6) location without perfusion (solid line) and with perfusion before (dashed line) and after (dash-dot line) the power increase.

B. Indirect temperature measurement

Fig. 8 and Fig. 9 demonstrate that by carefully choosing the feeding laser power it is possible to reach in the reference point almost the same temperature with and without perfusion (so in-, ex-vivo cases), while not exceeding the 100 °C limit elsewhere. Clearly, using the optimal power for the in-vivo case in an ex-vivo case would lead to maximum temperatures well above the 100 °C limit.

Even more interesting is that the effect of perfusion at the considered reference point can be evaluated in an indirect way by measuring the temperature at the FBG sensor position along the irradiating probe. Indeed, Fig. 10 shows that a sensor positioned along the irradiating probe is capable of discriminating the case of "under-heating" (when the process parameters of the ex-vivo case are use in an in-vivo ablation) from that of "correct heating". For example, in the considered case, the desired temperature slightly above 70 °C at the reference point is obtained only when the temperature read by the FBG sensor is about 100 °C. The location for the simulated temperature sensor is in correspondence of the middle of the fiber active length (i.e. at about 0.5 cm from the fiber tip) where the temperature distribution is approximately uniform, so that the gradient effect on the FBG measurement can be neglected at this stage [22].

These results, although still preliminary, are encouraging and allow opening the path to monitoring the ablation process in real-time without using sensors located in positions that require multiple percutaneous insertions. Starting from the particular geometry of the region under treatment, as obtained for example from an MRI or CT scan, through the model it is possible to design the probe irradiation pattern to match the tumor shape, find the optimal laser power to be used, and the temperature to be read by the FBG sensors in order to achieve the desired value in one or more reference points. Then, during the laser ablation process, the adherence to the hyperthermal treatment planning can be evaluated by continuously monitoring the temperature red by the FBG sensors.

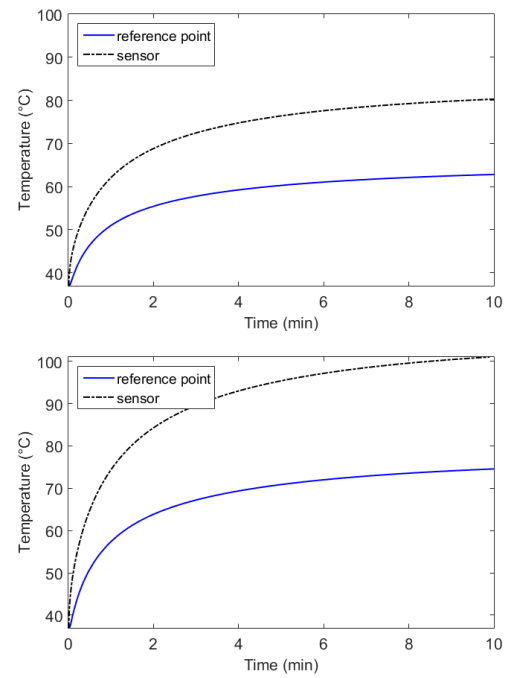

Fig. 10. Comparison of the temperature at the reference point (solid curve) and the FBG sensor location (dashed curve) for the in-vivo case at 4 W (above) and at 5.5 W (below) laser power.

V. Conclusion

The paper presented an analysis of the temperature distribution achievable in ex-vivo and in-vivo laser ablation procedures, showing that more effective outcomes require an accurate hyperthermal treatment planning that then must be strictly followed during the ablation procedure; this, in turn, requires the real-time mapping of the temperature distribution during the process. Indeed, it is not enough to characterize the effect of the applicator in ex-vivo cases since, having fixed a value of input power, ex-vivo LA treatments yield

higher maximum temperatures and broader cytotoxic areas with respect to in-vivo ablations. This is mainly due to the cooling effect of blood perfusion.

A model of the irradiating probe combined with a reliable map of the target anatomy, for instance as a result of a MRI/CT scan, is a fundamental tool to improve the treatment effectiveness, provided that then the adherence to the simulated ablation can be enforced during the actual treatment by controlling the predicted temperatures in selected reference points in the tumor mass with those read in real-time by sensors conveniently integrated in the applicator.

As a first step in this direction, this paper attempts at addressing the problem by simulating LA on a very simple geometrical domain, which considers a portion of liver tissue encompassing a blood vessel similar to the hepatic artery. The simulations showed that it is possible to relate the temperature read by the FBG sensors positioned along the irradiating fiber to that of another point chosen as reference in the geometrical domain.

References

[1] F.M. Di Matteo, P. Saccomandi, M. Martino, M. Pandolfi, M. Pizzicannella, V. Balassone, E. Schena, C.M. Pacella, S. Silvestri, and G. Costamagna,"Feasibility of EUS-guided Nd:YAG laser ablation of unresectable pancreatic adenocarcinoma," *Gastrointestinal Endoscopy*, 2018, (in press).

[2] K. Katsanos, L. Mailli, M. Krokidis, A. McGrath, T. Sabharwal, A. Adam, "Systematic review and meta-analysis of thermal ablation versus surgical nephrectomy for small renal tumours," *Cardiovascular and Interventional Radiology*, vol. 37, pp. 427-437, 2014.

[3] C. Pusceddu, B. Sotgia, R.M. Fele, and L. Melis,"Treatment of bone metastases with microwave thermal ablation,"*J Vasc Interv Radiol.*, vol. 24, pp 229-233, 2013.

[4] E. van Sonnenberg, W. McMullen, and L. Solbiati, *Tumor ablation: principles and practice*, 2nd ed. New York, USA: Springer, 2010.

[5] E.M. Knavel, and C.L. Brace, "Tumor ablation: common modalities and general practices," *Tech Vasc Interv Radiol.*, vol. 16, pp. 192–200, 2013.

[6] S. Sartori, F. Di Vece, F. Ermili, and P. Tombesi, "Laser ablation of liver tumors: an ancillary technique, or an alternative to radiofrequency and microwave?," *World J Radiol.*, vol. 9, pp. 91-96, 2017.

[7] G.G. Di Costanzo, G. Francica and C.M. Pacella, "Laser ablation for small hepatocellular carcinoma: State of the art and future perspectives," *World journal of hepatology.*, vol. 6, pp. 704–706, 2014.

[8] Y. Liu, R. Gassino, A. Braglia, A. Vallan, and G. Perrone, "Fibre probe for tumour laser thermotherapy with integrated temperature measuring capabilities," *El. Lett.*, vol. 52, pp. 798–800, 2016.

[9] J.J.W. Lagendijk and J. Mooibroek, "Hyperthermia treatment planning," in: G. Bruggmoser, W. Hinkelbein, R. Engelhardt, M. Wannenmacher, *Locoregional high-frequency hyperthermia and temperature measurement. Recent results in cancer research*, vol 101, Berlin, Germany: Springer, 1986.

[10] E. Schena, P. Saccomandi, and Y. Fong, "Laser ablation for cancer: past, present and future," *J. Funct. Biomater.*, vol. 8, 2017.

[11] M. de Greef, H.P. Kok, D. Correia, A. Bel, and J. Crezee, "Optimization in hyperthermia treatment planning: the impact of tissue perfusion uncertainty,", *Med Phys.*, vol. 39, pp. 4540–50, 2010.

[12] D. Tosi and G. Perrone, *Fiber-optic sensors for biomedical applications*, Boston, USA: Artech House, 2017.

[13] W. Chen, R. Gassino, Y. Liu, A. Carullo, G. Perrone, A. Vallan, and D. Tosi, "Performance assessment of FBG temperature sensors for laser ablation of tumors", *2015 IEEE Int. Symp. Medical Measurements and Applications* (MeMeA), pp.324?328, 2015.

[14] R. Gassino, Y. Liu, M. Olivero, A. Vallan, G. Perrone, and D. Tosi, "Toward the development of a distributed all-fiber temperature sensor for biomedical applications", *Proc. IEEE Int. Instrumentation and Measurement Technology Conference* (I2MTC), pp. 1?4, 2016.

[15] S. Korganbayev et al., "Detection of thermal gradients through fiber-optic Chirped Fiber Bragg Grating (CFBG): Medical thermal ablation scenario,"*Optical Fiber Technology*, vol. 41, pp. 48-55, 2018.

[16] P. Saccomandi et al., "Linearly chirped fiber Bragg grating response to thermal gradient: from bench tests to the real-time assessment during in vivo laser ablations of biological tissue,"*Journal of biomedical optics*, vol.22, pp. 1-9, 2017.

[17] Y. Liu, R. Gassino, H. Yu, A. Braglia, A. Vallan, G. Perrone, and D. Tosi, "Improved fiber probe for laser tissue ablation with integrated distributed temperature sensor," *Proc. SPIE*, vol. 9702, 2016.

[18] R. Gassino, Y. Liu, A. Vallan, M. Konstantaki, S. Pissadakis, and G. Perrone, "A fiber optic probe for tumor laser ablation with integrated temperature measurement capability," *J. Lightwave Technol.*, vol. 35, pp. 3447–3454, 2017.

[19] C. Rossmann and D. Haemmerich,"Review of temperature dependence of thermal properties, dielectric properties, and perfusion of biological tissues at hyperthermic and ablation temperatures," *Crit Rev Biomed Eng.*, vol. 42, pp. 467–492, 2014.

[20] H. Arkin, L. X. Xu and K. R. Holmes. "Recent developments in modeling heat transfer in blood perfused tissues," *IEEE Transactions on Biomedical Engineering*, vol. 41.2, pp. 97–107, 1994.

[21] Shibib, K. Salem, M. A. Munshid, and H.A. Lateef, "The effect of laser power, blood perfusion, thermal and optical properties of human liver tissue on thermal damage in LITT," *Lasers in Medical Science*, vol. 32, pp.2039–2046, 2017.

[22] R. Gassino, J. Pogliano, G. Perrone, and A. Vallan, "Issues and characterization of fiber Bragg grating based temperature sensors in the presence of thermal gradients," *Measurements*, 2018 (in press).